ADVANCED INDUCTION MOTOR DRIVE CONTROL WITH SINGLE CURRENT SENSOR

by

Evgenije M. ADŽIĆ[a*], Vlado B. POROBIĆ[a], Milan S. ADŽIĆ[b], and Zoran R. IVANOVIĆ[a]

[a]Faculty of Technical Sciences, University of Novi Sad, Novi Sad, Serbia
[b]College of Applied Sciences, University of Novi Sad, Subotica, Serbia

Original scientific paper
DOI:10.2298/TSCI150928027A

This paper proposes an induction motor drive control method which uses a minimal number of sensors, providing only DC-link current as a feedback signal. The improved DC-link current sampling scheme and modified asymmetrical switching pattern cancel the characteristic waveform errors which exist in all three reconstructed motor line-currents. Motor line-current harmonic content is reduced to an acceptable level, eliminating torque and speed oscillations which were inherent for conventional single sensor drives. Consequently, the use of single current sensor and line-current reconstruction technique is no longer acceptable only for low and medium performance drives, but also for the drives where obtaining a highly accurate, stable, and fast response is the priority. The proposed control algorithm is validated using induction motor drive hardware prototype based on TMS320F2812 digital signal processor.

Key words: *motor drive, induction motor, control design, digital control, vector control, sensorless control, single current sensor, current reconstruction method*

Introduction

Controlled electrical motor drives are the main driving force behind all automation systems in industry. In many applications such as cement, chemical, paper, metal, oil and gas industry they significantly contribute to the improved efficiency and reliability of manufacturing processes, simultaneously increasing energy savings and process safety. The most common electrical drives are induction motor (IM) drives, due to the great robustness and simple manufacturing process of this type of motor. Taking into account their wide distribution it is clear why in the past three decades, the IM controlled drives attract significant interest from academia and research centers around the world.

Generally, a great research effort is invested to continuously reduce the costs and to improve the drive reliability by finding ways to reduce the number of drive components to the minimum. This trend has now resulted in the fact that the size of the power converter is reduced by 70-80% compared to the 1980's, while the number of components dropped by 60-70%. Simultaneously, drive reliability, measured as the mean time between failures (MTBF), has increased about five times in the same period. This result was achieved primarily due to the

---

* Corresponding author, e-mail: evgenije@uns.ac.rs

enormous progress in the field of materials, switching components and microelectronics, but can also be partly attributed to the efforts invested in finding and improving motor control techniques [1].

This paper presents an improved IM control technique which is based on a drive with a minimal number of sensors. Due to the economy and reliability reasons, speed sensor is eliminated, as the first step [2]. Speed information is then determined indirectly, by measuring terminal currents and voltages [3-8]. Although direct measurement of motor terminal currents is the most effective way to achieve speed control without a sensor on the shaft, the use of additional components for measuring three-phase terminal currents (sensors, associated cables, conditioning circuitry) is not the most reliable and economically affordable solution. Therefore, the second step in the effort to increase reliability, is to substitute the three-phase motor current sensors with a single DC-link current sensor and a smart reconstruction algorithm [9]. However, taking into account the increasingly stringent safety measures and requirements involved, the application of a single DC-link current sensor in a control feedback loop is acceptable only if it can provide a robust and stable operation of the speed-sensorless drive.

The application of the conventional current reconstruction (CCR) method proves to be significantly lower in performances compared to the drives using direct line current measurement [10-15]. Lower performances are mainly the consequence of the unusual inaccuracy in the reconstructed current waveforms, which is explained in details in a previous paper [16]. The application of the CCR mechanism with two DC-link current samples in different time instants during the same switching period, in combination with PWM current ripple generates an error reflected in abrupt changes in reconstructed line-current waveforms. This error reflects further in *d-q* current components in a vector control algorithm, which can be observed in increased torque and speed oscillations. The accuracy of estimated speed is significantly reduced. Moreover, stability is seriously jeopardized in the situations when the current and speed controllers are tuned in an optimal way which is characteristic for high-performance drives.

This paper presents an original solution for CCR method improvement, which avoids weakening of controller parameters to reduce system dynamic, but at the same time eliminates an error and contributes to better control performances. A comparative analysis between the conventional and the proposed solution is given, in terms of the obtained motor line-current harmonics, and the developed torque and speed oscillations. The speed and *d-q* current control variables are also compared. Both stationary and transient analysis are included, with current and speed controller parameters tuned for a high-performance response. The proposed control algorithm is validated on two experimental setups: hardware-in-the-loop (HIL) and three-phase motor drive hardware prototype. The HIL results are given in previous paper [17], and the given justification results on real hardware prototype system are presented here.

Conventional current reconstruction method

The most reliable and cost effective three-phase motor line-current measurement is the use of only one current sensor placed in the power inverter DC-link. The block diagram of IM speed-sensorless drive with single current sensor and its control system is shown in fig. 1. Clarke and Park transformations (6, 7 and 4), space vector pulse-width modulator (SVPWM, 5), current controller (3), speed controller (9), and flux controller (2) are control blocks characteristic for vector-controlled drive [1]. Flux, angle and speed estimator (8) are native for speed-sensorless drives, when shaft-sensor is eliminated [2]. The core of the control scheme in a single sensor drive are the blocks for three-phase current reconstruction (10) and modified SVPWM (5) with the task to support critical cases in reconstruction mechanism. The flux estimator used belongs to the class of advanced estimators covering a wide range of speed [18]. The applied speed estimator is a simple open-loop estimator [2, 3] which uses flux speed obtained by conventional phase-locked-loop (PLL) method [19]. However, the main focus of this paper is not the speed estimation itself, but the three-phase current reconstruction method and its influence on the given speed-sensorless drive.

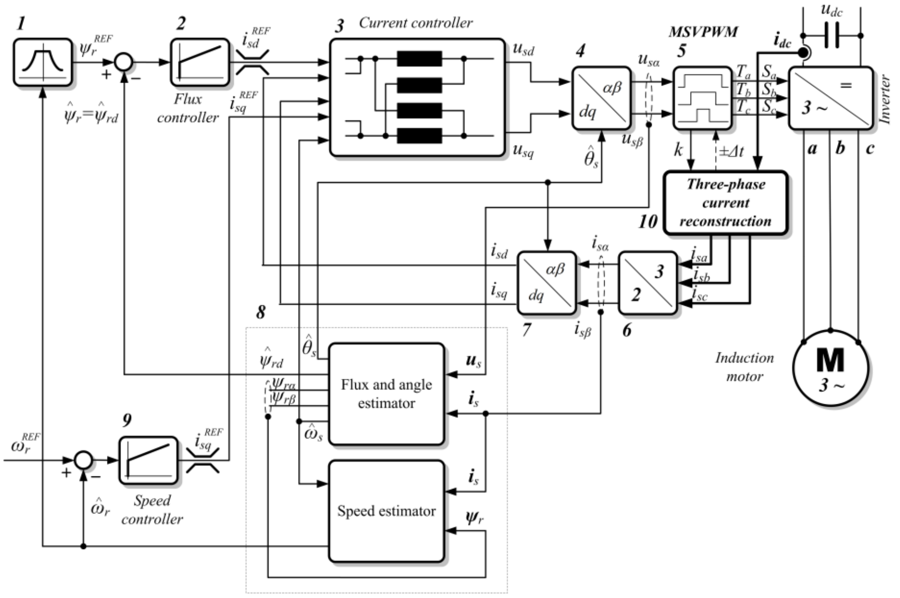

Figure 1. Control system of vector-controlled induction motor drive with single current sensor

Due to the topology of the three-phase inverter and selected switching modulation (SVPWM), it is possible to reconstruct motor phase-currents from the measured DC-link current [9]. In each switching period, DC-link current includes information about two motor line-currents while the remaining third current could be reconstructed taking into account that the sum of the line currents is equal to zero. Figure 2 shows an example and details of CCR principle, where switching PWM signals S_A, S_B, and S_C for upper inverter switches are arranged defining the output voltage vector in the first SVPWM sector ($k = 1$). Two DC-link current samples (i_h and $-i_l$) are taken at the strategic moments (T_{samp1} and T_{samp2}) which are precisely synchronized regarding the middle of switching PWM period (*TRIG*) and according to the beginning of the active voltage vectors, as shown in fig. 2. Here, current sample (i_h) during the active voltage vector with only one upper switch turned-on is equal to the phase current i_a, while current sample ($-i_l$) during the active voltage vector with two upper switches turned-on is equal to the inverted value of motor phase current i_c. A similar analysis could be performed for other SVPWM sectors that yield to complete current reconstruction algorithm, given in tab. 1. The relationship between DC-link current and three-phase currents does not depend on the power flow direction, so the reconstruction method can be applied for both motoring and generating operational regime of the induction machine.

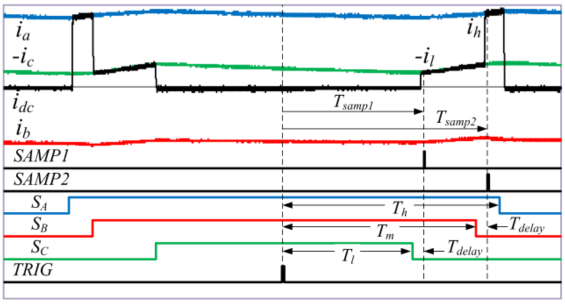

Figure 2. The DC-link current sampling principle in conventional current reconstruction method

Table 1. Relationship between motor line-currents and DC-link current samples

Sector (k)	Switching states (S_a, S_b, S_c)	Line current i_a	Line current i_b	Line current i_c
1	$V_1=(1,0,0)$ $V_2=(1,1,0)$	i_h	$-(i_h+i_l)$	$-i_l$
2	$V_2=(1,1,0)$ $V_3=(0,1,0)$	$-(i_h+i_l)$	i_h	$-i_l$
3	$V_3=(0,1,0)$ $V_4=(0,1,1)$	$-i_l$	i_h	$-(i_h+i_l)$
4	$V_4=(0,1,1)$ $V_5=(0,0,1)$	$-i_l$	$-(i_h+i_l)$	i_h
5	$V_5=(0,0,1)$ $V_6=(1,0,1)$	$-(i_h+i_l)$	$-i_l$	i_h
6	$V_6=(1,0,1)$ $V_1=(1,0,0)$	i_h	$-i_l$	$-(i_h+i_l)$

Difficulties with conventional current reconstruction method

The DC-link current sampling error

Practical difficulties with DC-link current sampling occur when a switching PWM period contains narrow active voltage vectors ($\vec{V}_k$, $k = 1...6$), which happens in two common cases [10]. The first case is a situation where the reference voltage vector passes between SVPWM sectors ($k \rightarrow k \pm 1$), and when PWM signal duty cycle values for the two inverter legs are almost equal. Figure 3 shows an example, recorded during the experiments on the HIL setup, when the voltage vector passes between the first ($k = 1$) and the second sector ($k = 2$) and when it is possible to reconstruct only one line current, $-i_c$. Voltage vector $\vec{V}_2$ ($S_a = 1$, $S_b = 1$, $S_c = 0$) is long enough to sample DC-link current, i_{dc}, which is in the first sector equal to the inverted value of line current, $i_{dc}(T_{samp1}) = -i_c$. Line current i_a is unobservable, due to the short active voltage $\vec{V}_1$ ($S_a = 1$, $S_b = 0$, $S_c = 0$). Instead of reading line current i_a, the second DC-link current sample measure zero current, $i_{dc}(T_{samp2}) = 0$, when zero voltage $\vec{V}_0$ ($S_a = 0$, $S_b = 0$, $S_c = 0$) is applied. This is always the case in normal operation due to the reference voltage vector rotation, regardless of the modulation index value. The second critical situation is a low modulation index, when both active vectors are present for a short time. The PWM duty cycles values for all three inverter legs are almost the same and around 50%. DC-link current sampling windows in the frame of both active vectors are not sufficiently long for reliable DC-link current measurement.

Line-current information could not be obtained without modifying PWM switching pattern in order to provide long enough voltage vectors.

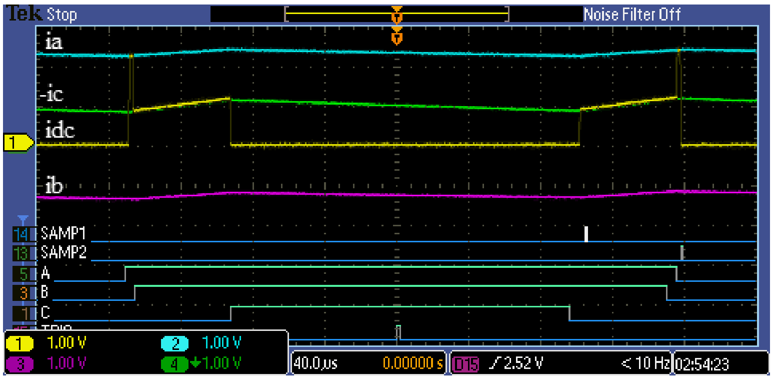

Figure 3. Example of critical case for line-current reconstruction – voltage vector passes between sectors (*k* = *1*→*2*)

Figure 4 shows the resulting three-phase reconstructed currents if the originally symmetrical PWM switching scheme is applied, without the mechanism for obtaining the minimal width of active voltage vectors. There is a significant reconstructed current waveform distortion in critical periods. The reconstructed phase-currents are useless as current feedback in speed-sensorless vector-controlled drive, because they will yield to flux/speed estimation and current/speed controller unstable operation. Large deviation of the reconstructed currents (i_a^{REC}, i_b^{REC}, i_c^{REC}) from the actual current values (i_a, i_b, i_c) can be noticed in the area between different voltage sectors (*Sector*). The reconstructed currents are even more distorted when low modulation index is applied. To overcome these difficulties it is necessary to perform one of the suggested mechanism for reliable DC-link current measurement by modifying the originally symmetrical PWM voltage pattern [10-15, 20]. The proposed modified unsymmetrical PWM switching pattern which reliably obtains DC-link current samples and can also function in critical cases when longer active vectors are needed, is given in the next section.

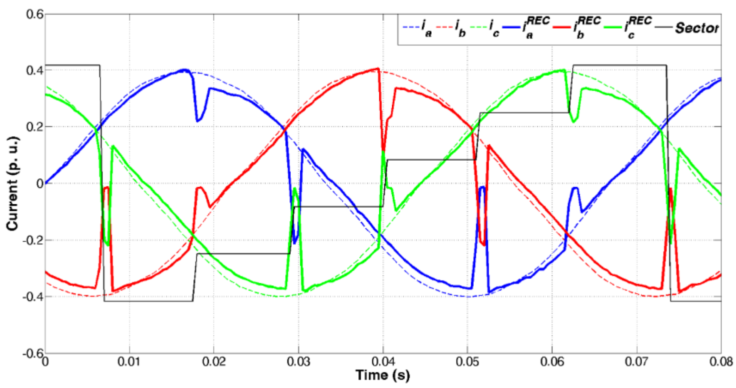

Figure 4. Distortion in reconstructed currents without using modified PWM switching pattern

Reconstructed motor line current waveform error due to current ripple

Regardless of the selected modified PWM switching pattern for line-current reconstruction, the end results cannot be the line-currents sampled in the middle of the PWM period. Due to the nature of the reconstruction method, two observable line-currents cannot be sampled simultaneously, but each is sampled when available and thus with a certain time-displacement between the two samples. As a result, these two values are phase-shifted differently from the middle point of the PWM period, in which the average PWM value of the line-current, i_x^{AV} ($x = a, b, c$), is located (fig. 5). Each current sample deviates from its PWM average value, which can be qualitatively represented with the current ripple error, Δ.

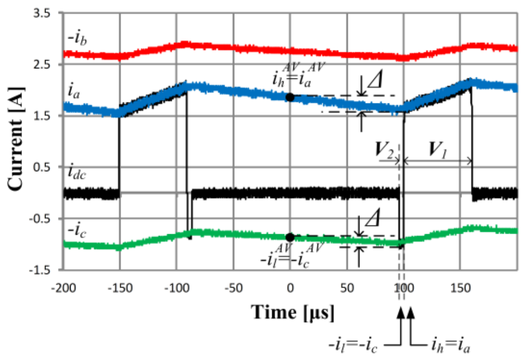

Figure 5. The PWM current ripple error (Δ) in sampled line-currents – case when reference voltage vector is at the beginning of the first sector

A combination of time-displacement of the two line-current samples and current PWM ripple, for different positions of rotating reference voltage vector, produces a particularly shaped error of the reconstructed line-current. This kind of error is uncovered and explained in detail in [16]. Table 2 and fig. 6 give an overall view of the complex, ripple-caused error in the reconstructed line-current (i_b for example). The approximate errors are given for each sector, and especially for the reference voltage vector position at the beginning, middle and end of the sector. It is clear that two abrupt excursions in the current signal can be expected during one period of fundamental output voltage. The ripple-induced error exhibits steps of 3·Δ amplitude twice per period (transitions between sectors 1→2 and 3→4 for line-current i_b) and it practically produces an offset section. For the other two line-currents, transition offsets would appear at different positions (1→2 and 5→6 for i_a, and 3→4 and 5→6 for i_c current). Figure 6 shows the experimental results in open-loop control that demonstrate the erroneous offset of the two sectors, with the measured (i_b) and reconstructed motor line-current (i_b^{REC}). The line-current waveform error shown directly reflects on the rotating reference frame current components, *d-q* currents, producing 3rd and 6th harmonic jitter. Furthermore, the error propagates through the whole control system, producing unstable operation of all estimators and controllers. A higher order low-pass or notch filters are usually introduced in the control system that remove the ripple caused error in *d-q* currents, but at the price of drastically reduced system dynamic. This is mainly the reason why current recon-

Table 2. Ripple error in reconstructed current (i_b)

Sector (k)	Sector part			Transition offset
	Begin	Middle	End	
1	i_b^{AV}	$i_b^{AV}-\Delta$	$i_b^{AV}-2\Delta$	3Δ
2	$i_b^{AV}+\Delta$	i_b^{AV}	$i_b^{AV}-\Delta$	*0*
3	$i_b^{AV}-\Delta$	i_b^{AV}	$i_b^{AV}+\Delta$	–3Δ
4	$i_b^{AV}-2\Delta$	$i_b^{AV}-\Delta$	i_b^{AV}	Δ
5	$i_b^{AV}+\Delta$	$i_b^{AV}+\Delta$	$i_b^{AV}+\Delta$	*0*
6	$i_b^{AV}+\Delta$	$i_b^{AV}+\Delta$	$i_b^{AV}+\Delta$	–Δ

struction method was usually applied in low-performance drives. For its application in high-performance drives, more advanced techniques for current reconstruction has to be included, as proposed in this paper.

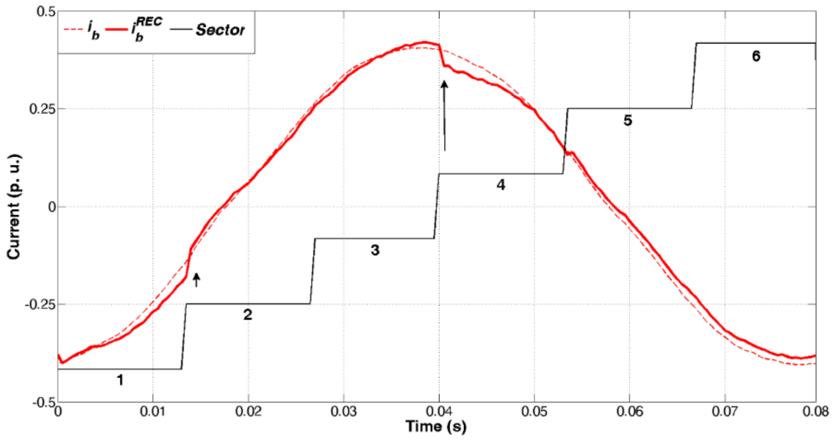

Figure 6. Reconstructed line current (i_b^{REC}) in comparison to the directly measured line current (i_b) – conventional reconstruction method

The proposed current reconstruction method

The basic idea suggested in this paper represents an improvement of the method explained in [10], which used the line-currents measured in both halves of the naturally symmetrical PWM switching period. The method proposed in [10] is based on the sampling of the DC-link current in the center of the active voltage vectors four times during one PWM period and the calculation of the two available line-current values by averaging the samples from two matching vector pairs (fig. 7).

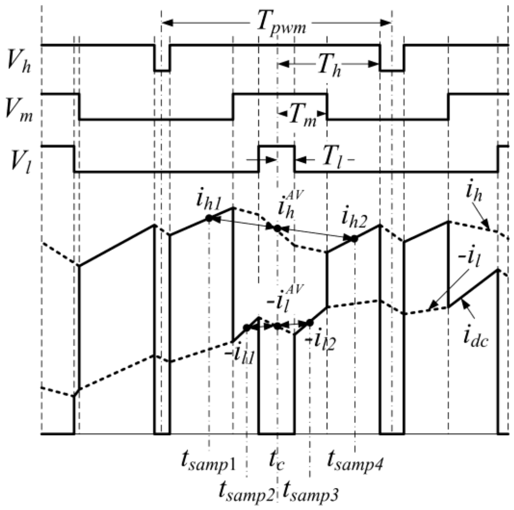

Figure 7. Improved sampling scheme for current reconstruction method with four current samples in one PWM period

This approach provides a synchronous meas-urement of all three line-currents, referred to the center of a PWM period. It effectively cancels the error due to current ripple in the reconstructed line-currents and eliminates the current samples' mutual phase-shift. Besides its simplicity, this met-hod is completely insensitive to machine parameter variances. However, the critical cases of a reference voltage vector passing between voltage sectors or with a low modulation index are neglected and not considered in [10]. This would cause highly distorted reconstructed currents (fig. 4) and unstable drive operation, as explained in the section *DC-link current sampling error*.

Considering the high PWM switching fre-quencies, and the usually employed electrical motors, one can conclude that there is no need for the very high current control-loop sampling rate at the PWM level. This fact allows us to record line-current information on the lagging (right) side of one PWM period and then on the leading (left) side of the subsequent PWM period and calculate the available line-currents by simple averaging of the corresponding recorded values. In this way, all three estimated line-currents would be referred to the same instant reflecting the average current value in two consecutive PWM periods.

Figure 8 shows the DC-link current (i_{dc}) and motor line currents (i_a, i_b, i_c) during two consecutive PWM periods and the details related to the proposed method. Sampling signals *SAMP1* and *SAMP4* are the triggers for the measurement of DC-link current in two consecutive PWM periods during matching active voltage vectors defined with only one inverter switch turned-on (in shown sector 1, S_a=1). *SAMP1* samples DC-link current (i_{ho}) at the beginning of the active voltage vector in the odd PWM period, and *SAMP4* at the end of the active vector (i_{he}) in the even PWM period. Similarly, sampling signals *SAMP2* and *SAMP3* are the triggers for the measurement of DC-link current at the beginning ($-i_{lo}$) and at the end ($-i_{le}$) of matching active voltage vectors defined with two upper switches turned-on (in sector 1, S_a=1 and S_b=1).

The line currents at the time instant representing the average values in two consecutive PWM periods can be obtained using simple calculation:

$$i_l^{AV} = -\frac{i_{dc}(SAMP2)+i_{dc}(SAMP3)}{2} = -\frac{i_{lo}+i_{le}}{2}$$

$$i_h^{AV} = \frac{i_{dc}(SAMP1)+i_{dc}(SAMP4)}{2} = \frac{i_{ho}+i_{he}}{2} \tag{1}$$

$$i_m^{AV} = -\left(i_l^{AV}+i_h^{AV}\right)$$

It remains to assign the resultant currents i_h^{AV}, i_m^{AV}, and i_l^{AV} to motor line-currents i_a, i_b and i_c depending on the actual sector number as in conventional case (tab. 1).

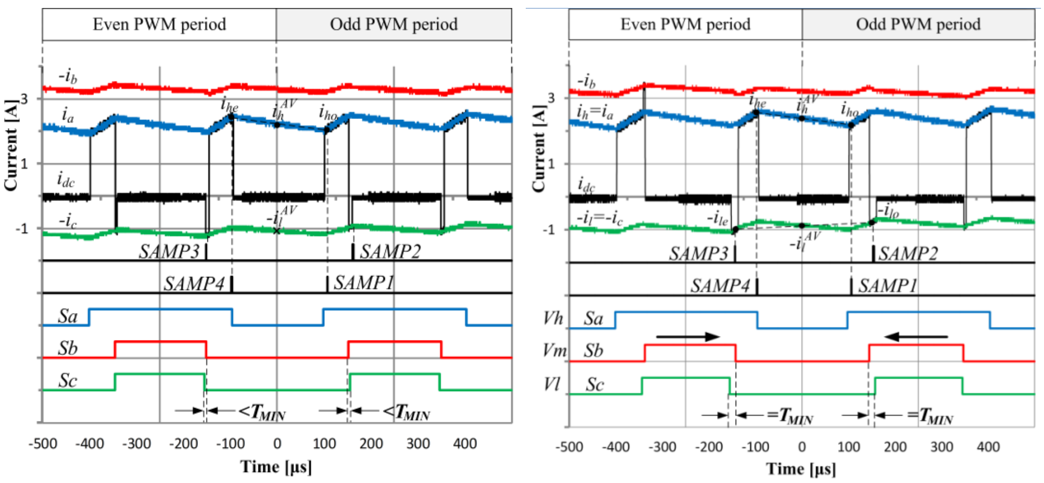

(a) (b)

Figure 8. (a) Proposed DC-link current sampling scheme, and (b) modified PWM pattern for improved line current reconstruction

The proposed sampling method enables us to improve the PWM pattern control in order to account for critical cases. The suggested switching method modifies PWM signals associated with the middle (V_m) and highest (V_h) voltage commands. Both signals are shifted in the right direction, considering even PWM periods, to form active vectors with minimal width T_{MIN} for reliable DC-link current measurement. Similarly, in odd PWM periods, both PWM signals are left-shifted to provide sampling window width of T_{MIN} fig. 8(b). The method is explained only for even PWM periods, because the procedure is also valid for odd periods, but in the reverse direction.

Firstly, if needed, PWM signal V_m is right–shifted by time:

$$\Delta T_{vector1} = T_{MIN} - (T_m - T_l) \tag{2}$$

Active time intervals of PWM signal V_m during lagging and leading half-periods in even PWM cycles should be updated to new values, T_{m2} and T_{m1}, respectively:

$$T_{m2} = T_h + \Delta T_{vector1}$$

$$T_{m1} = T_m - \Delta T_{vector1} \tag{3}$$

This case is shown in fig. 8(b). Then, the second active vector duration has to be calculated and if needed, PWM signal V_h has to be right-shifted. Signal V_h width in lagging PWM half-period has to be extended, and in leading half-period reduced, to new values T_{h2} and T_{h1}:

$$\Delta T_{vector2} = T_{MIN} - (T_h - T_{m2})$$

$$T_{h2} = T_h + \Delta T_{vector2}$$

$$T_{h1} = T_h - \Delta T_{vector2} \tag{4}$$

Experimental results

In order to validate the effectiveness and reliability of the proposed control algorithm, HIL emulator is used in the early stage of verification [17]. However, HIL testing does not cover all the complexities and phenomena which appear in real systems. To further confirm the usefulness of the proposed method, a prototype drive experimental set-up shown in fig. 9 was used. The induction motor (rated power 1.1 kW, rated voltage 380 Vrms, rated current 2.8 Arms, Y, 4-pole, rated speed 1410 rpm, R_s = 9.173 Ω, R_r = 6.422 Ω, L_m = 320.3 mH, L_s = 18.89 mH, L_r = 17.28 mH) was controlled with a 3-phase voltage inverter, based on digital signal processor TMS320F2812.

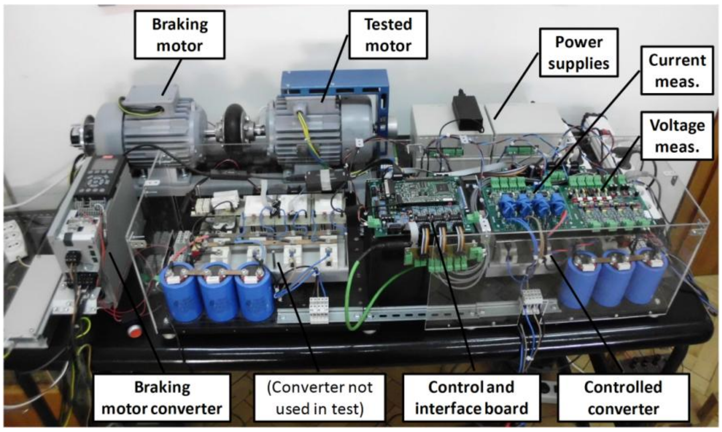

Figure 9. Experimental induction motor drive used in tests

The adopted controller base values, which are relevant for interpreting the experimental results, are: base speed 2000 rpm and base current 7 A. The same motor type controlled in torque mode with an industrial frequency converter was used for setting the desired load torque reference.

Figure 10 compares the dynamic speed response of the sensorless IM drive with both the conventional and the proposed current reconstruction method for a ramp-change (0.4 second) in the speed reference from 100 rpm (0.05 p. u.) to 750 rpm (0.375 p. u.). The motor was lightly loaded (1.1 Nm, 15% rated), which resulted in a low current rms value and in the significantly distorted reconstructed current waveforms. In addition to the measured and the estimated speeds, ω_r and ω_r^{EST}, fig. 10 also shows *d-q* current references, i_d^{REF} and i_q^{REF}, and *d-q* components of the actual measured motor line-currents, i_d and i_q. In a vector-controlled drive current i_d directly determines motor flux, and current i_q determines motor electromagnetic torque. In that manner, the oscillations in *d-q* currents directly indicate the oscillations in motor flux and torque.

In the control system with a conventionally reconstructed line-current feedback, there are significant oscillations in the obtained motor line-currents *d-q* components compared to the case where the proposed current reconstruction is used. Even more importantly, there is a noticeable offset in i_q current fig. 10(a), which is mostly canceled using the proposed algorithm, fig. 10(b).

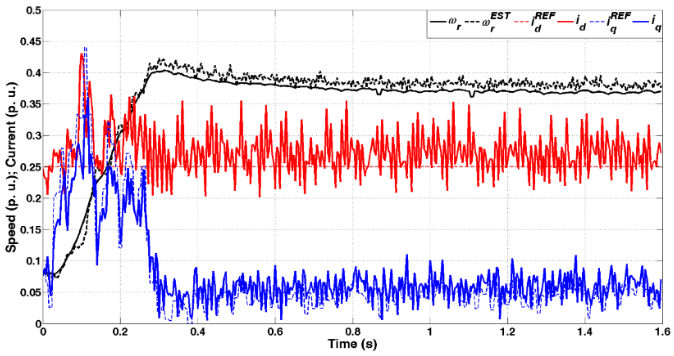

(a) ***Using conventional current reconstruction method***

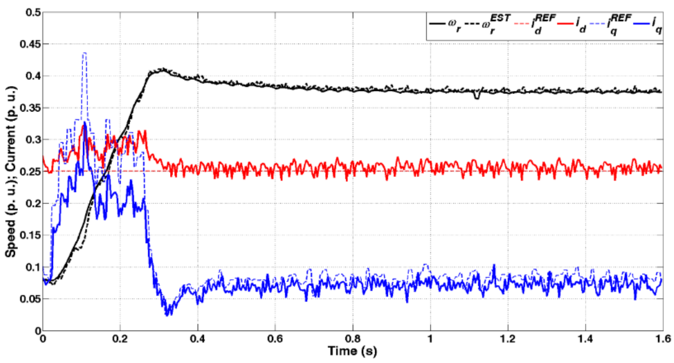

(b) ***using proposed current reconstruction method***

Figure 10. Dynamic response with change in speed reference from 0.05 p. u. to 0.375 p. u., and 15% rated load

Taking into account that the presence of offsets in the current signals (measured or reconstructed) can negatively influence the flux and speed estimation [21-24], the advantages of the proposed method are evident. In that respect, fig. 11 illustrates the current offset influence on the speed estimation and steady-state speed error. The elimination of *d-q* current offset in the proposed system caused a steady-state speed error (5 rpm, 0.0025 p. u.) which is four times smaller than the conventional system (20 rpm, 0.01 p. u.). Since current reconstruction and current control loop dynamics are an order of magnitude faster than the speed control loop, the reconstruction method does not affect the speed dynamic performance of the drive. However, smoother and more stable response immediately after a ramp-change in speed reference is noticeable in the case of the proposed control system (fig. 10).

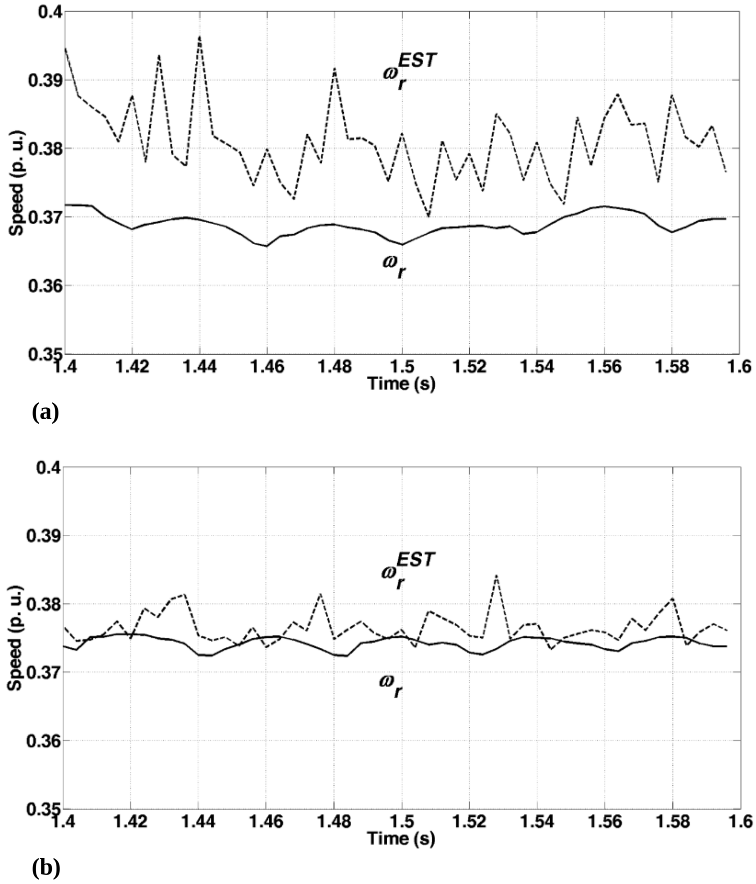

Figure 11. Steady-state speed error for speed reference 0.375 p. u. and 15% rated load: (a) with conventional current reconstruction, (b) with proposed current reconstruction

The main improvements with the proposed method over the conventional method for motor line-current reconstruction could be observed throughout the steady-state *d-q* current response given in figs. 12 and 13. Figure 12 gives the results for 15% rated load and fig. 13 shows the results for rated load. It is evident that *d-q* currents (reconstructed i_d^{REC} and i_q^{REC}, but also actual measured i_d and i_q) oscillate significantly around the average value (3rd and 6th harmonic) and have incorrect average values (offset). Figures 12(b)-13(b) confirm that limited and acceptable 3rd and 6th harmonic jitter in the *d-q* current components are achieved. More importantly, the offset error, particularly evident in the q-current component is almost completely eliminated using the proposed method. In the considered cases, a lower q-component average value of the reconstructed currents than referenced, resulted in a higher applied output voltage for the same load torque and flux, as compared to the proposed control system. This could be important for higher reference speed than nominal, *i.e.* in field weakening region.

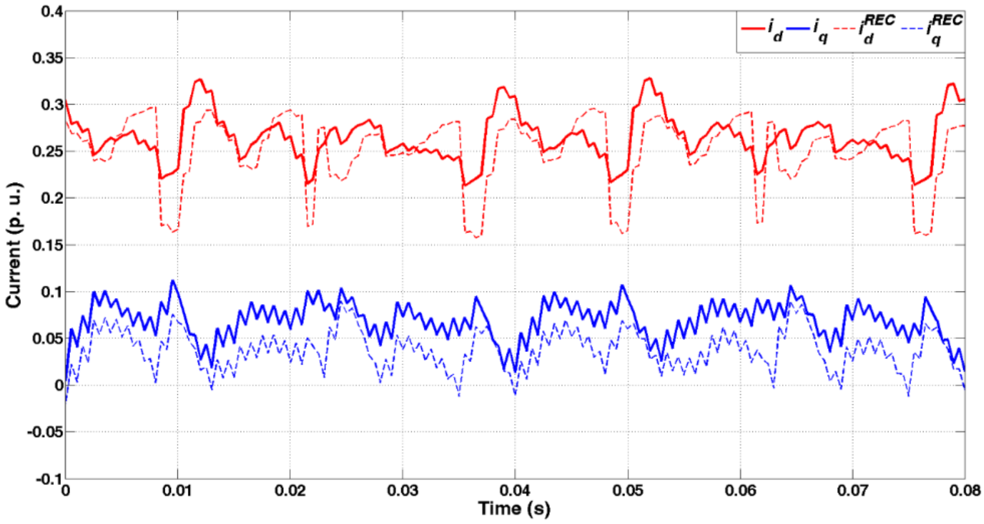

(a) ***Using conventional current reconstruction method***

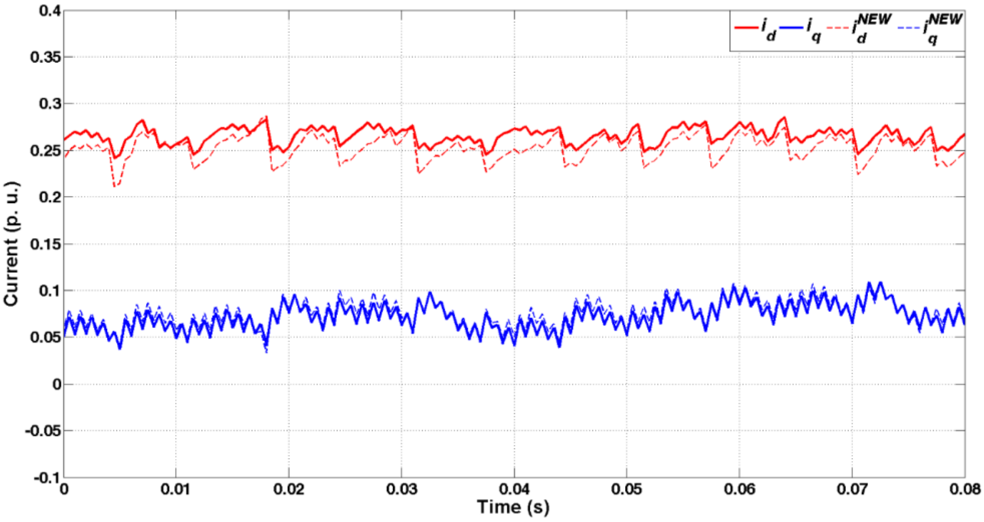

(b) ***Using proposed current reconstruction method***

Figure 12. Steady-state *d-q* current response for speed reference 0.375 p. u. and 15% rated load

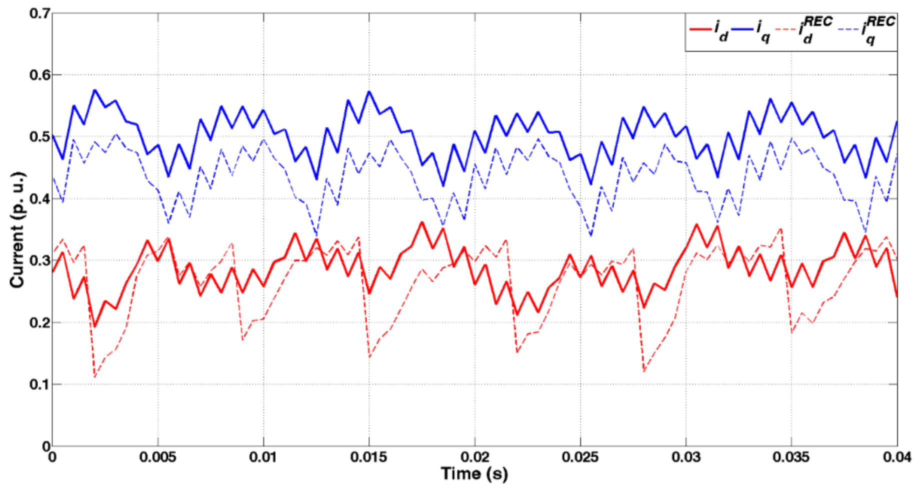

(a) ***Using conventional reconstruction method***

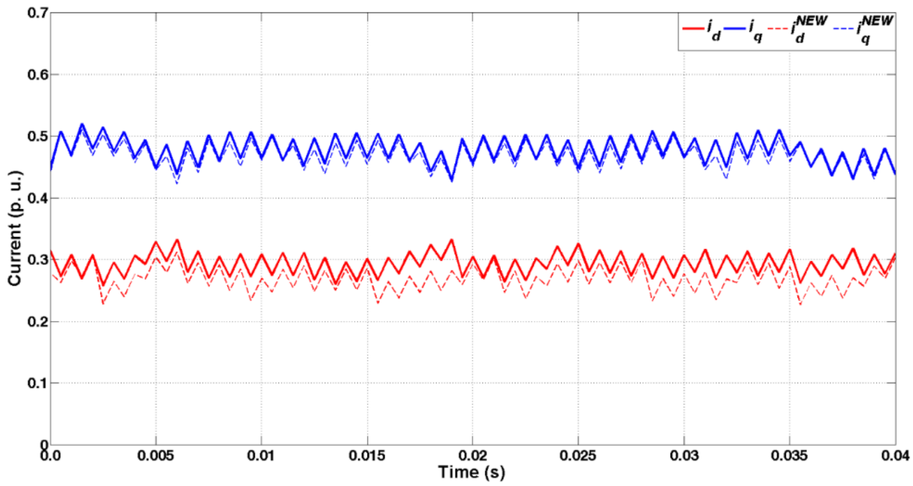

(b) ***Using proposed current reconstruction method***

Figure 13. Steady-state *d-q* current response for rated speed reference 0.705 p. u. and rated load 7.45 Nm

Finally, figs. 14 and 15 give the comparative results of motor line-current harmonic analysis for different situations when control algorithm uses the current feedbacks which are directly measured, reconstructed with the conventional method, and with proposed method. Harmonic analysis was conducted for two load torque values, 1.5 Nm (20% rated) and 7.45 Nm (rated), both for speed reference 300 rpm (0.1 p. u.). The results are normalized and given relative regard to the fundamental harmonic. Of interest were the harmonic values at lower frequencies, which can significantly influence the current and speed control structure and could yield to lower control performances. Therefore, figs. 14 and 15 show harmonic content from 2nd to 7th harmonic (and collectively in the first column), which were dominant in the conventional control structure, and up to four times reduced in the proposed system. Current harmonic distortion in the proposed system is comparable to the case when currents were directly measured. The obtained results prove that lower order harmonics were eliminated and that quality was improved thanks to the selected control strategy.

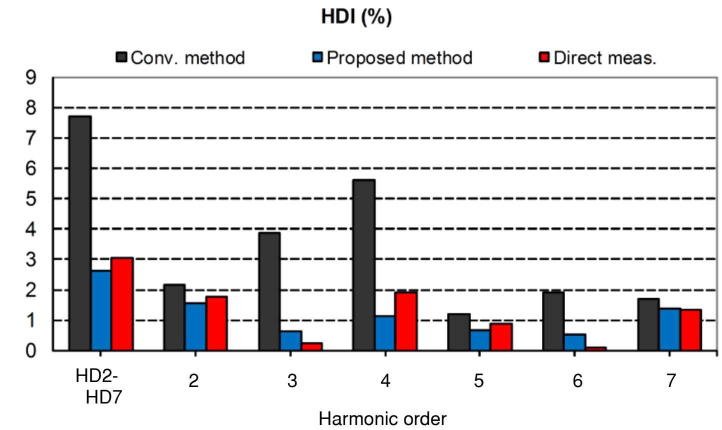

Figure 14. Lower order harmonic content for reference speed 300 rpm and 20% rated load torque

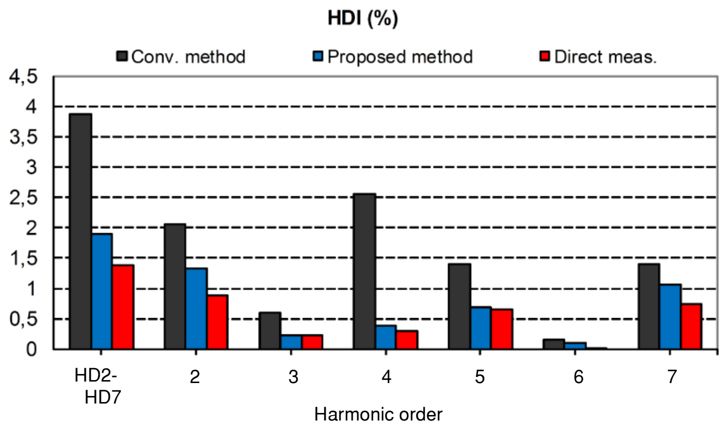

Figure 15. Lower order harmonic content for reference speed 300 rpm and rated load torque

Conclusions

This paper proposes improved current reconstruction algorithm which is suitable for integration in the standard speed-sensorless vector-controlled IM drives. The proposed solution is completely independent on the machine model and parameters. It uses averaging of totally four DC-link current samples in two consecutive PWM periods, which significantly reduces the phase error and characteristic harmonics in the *d-q* current components. The average DC-link samples are referred to the same time instant which yields the reconstructed line current waveforms which are almost the same as the actual measured values.

The obtained results verify that the proposed method reduces motor current harmonics, as well as torque and speed oscillations to the acceptable level in the case when only one current sensor is used, and in the conditions where all controller and estimator parameters are set for high performance response. Now, single sensor and current reconstruction is not only acceptable for low and medium performance drives, but it could be helpful in high-performance drives where accomplishing a highly accurate, stable and fast response is the priority.

Future work can be focused on detailed analysis of the acoustic noise introduced by different current reconstruction methods and on the application of the proposed method in more complex systems with high-reliability demand such as the wind turbine system explained in [25] (machine in generating regime).

Acknowledgment

This research was partially co-funded by the Ministry of Education, Science and Technological Development of the Republic of Serbia under contract No. III 042004 and by the Provincial Secretariat for Science and Technological Development of AP Vojvodina under contract No. 114-451- 3508/2013-04.

References

[1] Bose, B., *Power Electronics and Motor Drives – Advances and Trends,* Elsevier Inc., London, 2006
[2] Vas, P., *Sensorless Vector and Direct Torque Control,* Oxford University Press Inc., New York, USA, 1998
[3] Holtz, J., Sensorless Control of Induction Motor Drives, *Proceedings,* IEEE, 2002, Vol. 90, No. 8, pp. 1359-1394
[4] Peng, F. Z., Fukao, T., Robust Speed Identification for Speed Sensorless Vector Control of Induction Motors, *IEEE Tran. Ind. Appl.*, *30* (1994), 5, pp.1234-1239
[5] Joetten, R., Maeder, G., Control Methods for Good Dynamic Performance Induction Motor Drives Based on Current and Voltage as Measured Quantities, *IEEE Trans. on Ind. Appl.*, *IA-19* (1983), 3, pp. 356-363
[6] Hurst, K. D., Habetler, T. G., Sensorless Speed Measurement Using Current Harmonic Spectral Estimation in Induction Machine Drives, *IEEE Trans. Pow. Elec.*, *11* (1996), 1, pp. 66-73
[7] Jansen, P. L., Lorenz, R. D., Transducerless Position and Velocity Estimation in Induction and Salient AC Machines, *IEEE Trans. on Ind. Appl.*, *31* (1995), 2, pp. 240-247
[8] Lascu, C., *et. al.*, A Class of Speed-Sensorless Sliding-Mode Observers for High-Performance Induction Motor Drives, *IEEE Trans. on Ind. Electron.*, *56* (2009), 9, pp. 3394-3403
[9] Green, T. C., Williams, B. W., Control of Induction Motors Using Phase Current Feedback Derived from the DC Link, *Proceedings,* EPE'89, 1989, Vol. 3, pp. 1391-1396
[10] Blaabjerg, F., *et al.*, Single Current Sensor Technique in the DC Link of Three-Phase PWM-VS Inverters: A Review and a Novel Solution, *IEEE Trans. Ind. Appl.*, *33* (1997), 5, pp. 1241-1253
[11] Zhang, C., Lin, F., A Single Current Sensor Control Technique for Induction Motors, *Proceedings,* PowerCon, International Conference on Power System Technology, Kunming, China, 2002, Vol. 4, pp. 2290-2293
[12] Kim, H., Jahns, T. M., Phase Current Reconstruction for AC Motor Drives Using a DC Link Single Current Sensor and Measurement Voltage Vectors, *IEEE Trans. Power Electron.*, *21* (2006), 5, pp. 1413-1419
[13] Ha, J. I., Voltage Injection Method for Three-Phase Current Reconstruction in PWM Inverters Using a Single Sensor, *IEEE Trans. on Power Electron.*, *24* (2009), 3, pp. 767-775
[14] Ha, J. I., Current Prediction in Vector-Controlled PWM Inverters Using Single DC-Link Current Sensor, *IEEE Trans. on Ind. Electron.*, *57* (2010), 2, pp. 716-726
[15] Gu, Y., *et. al.*, Switching-State Phase Shift Method for Three-Phase-Current Reconstruction With a Single DC-Link Current Sensor, *IEEE Trans. on Ind. Electron.*, *58* (2011), 11, pp.5186-5194
[16] Marčetić, D., Adžić, E., Improved Three-Phase Current Reconstruction for Induction Motor Drives With DC-Link Shunt, *IEEE Ind. Electron.*, *57* (2010), 7, pp. 2454-2462

[17] Adžić, E., *et. al.*, Sensorless Vector Control of Induction Motor with Current Reconstruction Method, *Proceedings*, 7th International Conference on Engineering and Technology – ICET, Phuket, Thailand, 2015
[18] Lascu, C., *et. al.*, A Modified Direct Torque Control for Induction Motor Sensorless Drive, *IEEE Trans. on Ind. Electron.*, *36* (2000), 1, pp. 122-130,
[19] Comanescu, M., Xu, L., An Improved Flux Observer Based on PLL Frequency Estimator for Sensorless Vector Control of Induction Motors, *IEEE Trans. on Ind. Electron.*, *53* (2006), 1, pp. 50-56
[20] Liu, G., *et. al.*, Procedure for Measuring the Current in each Phase of a Three-Phase Device via Single Current Sensor, US Patent 6735537 B2, USA, 2004.
[21] Chung, D. W., Sul, S. K., Analysis and Compensation of Current Measurement Error in Vector-Controlled AC Motor Drives, *IEEE Trans. on Industry Applications*, *34* (1998), 2, pp.340-345
[22] Choi, J. W., *et. al.*, Novel Periodic Torque Ripple Compensation Scheme in Vector Controlled AC Motor Drives, *Proceedings*, 13th Annual Conference on Applied Power Electronics (APEC), Anaheim, Cal., USA, 1998, Vol. 1, pp. 81-85
[23] Jung, H.S., *et. al.*, Diminution of Current-Measurement Error for Vector-Controlled AC Motor Drives, *IEEE Trans. on Industry Applications*, *42* (2006), 5, pp. 1249-1256
[24] Hur, N., *et. al.*, Sensorless Vector Control in Presence of Voltage and Current Measurement Errors by Dead-Time, *Proceedings*, 32nd Industry Applications Conference - IAS, New Orleans, La., USA, 1997, Vol. 1, pp. 433-438
[25] Dumnić, B., *et. al.*, An Improved MRAS Based Sensorless Vector Control Method for Wind Power Generator, *Journal of Applied Research and Technology – JART*, *10* (2012), 5, pp. 687-697

Paper submitted: September 28, 2015
Paper revised: December 17, 2015
Paper accepted: December 29, 2015